

Multiwavelet-like bases for high quality image interpolation

Koichi Ichige^a, Thierry Blu^b and Michael Unser^b

^a Department of Electrical and Computer Engineering, Yokohama National University,
Yokohama 240-8501, Japan.

^b Biomedical Imaging Group, Swiss Federal Institute of Technology Lausanne (EPFL),
CH-1015 Lausanne, Switzerland.

ABSTRACT

We present a simple but generalized interpolation method for digital images that uses multiwavelet-like basis functions. Most of interpolation methods uses only one symmetric basis function; for example, standard and shifted piecewise-linear interpolations use the “hat” function only. The proposed method uses q different multiwavelet-like basis functions. The basis functions can be dissymmetric but should preserve the “partition of unity” property for high-quality signal interpolation. The scheme of decomposition and reconstruction of signals by the proposed basis functions can be implemented in a filterbank form using separable IIR implementation. An important property of the proposed scheme is that the prefilters for decomposition can be implemented by FIR filters. Recall that the shifted-linear interpolation requires IIR prefiltering, but we find a new configuration which reaches almost the same quality with the shifted-linear interpolation, while requiring FIR prefiltering only. Moreover, the present basis functions can be explicitly formulated in time-domain, although most of (multi-)wavelets don’t have a time-domain formula. We specify an optimum configuration of interpolation parameters for image interpolation, and validate the proposed method by computing PSNR of the difference between multi-rotated images and their original version.

Keywords: interpolation, linear interpolation, filterbank, wavelet

1. INTRODUCTION

Interpolation is one of the standard operations in digital signal/image processing.^{1,2} In most of high quality interpolation methods, input signals are first transformed into weight parameters of the given basis function by prefiltering (decomposing). After that a continuous signal is reconstructed as a weighted sum of shifted basis functions by reconstruction filtering. The inherent problem of those algorithms with prefiltering is that the prefilter often makes Gibbs phenomenon (oscillations) which is favored by the fact that the prefilter is generally given as an IIR filter. A way to reduce Gibbs oscillations would be to employ multiple generators (basis functions) instead of one. This is because the prefilters for multiple generators can be FIR filters for a certain range of parameters values.

In the first part of this paper, we will be investigating FIR interpolation using multiple generators. Then we will pay a special attention to the family of piecewise-linear interpolation because of its simplicity and low computational cost. Among the multitude of algorithms that have been proposed, piecewise-linear interpolation is still the method of choice for many applications due to its low computational cost.

Recently, two of the present authors have proposed shifted-linear interpolation⁴ which greatly improves the quality of reconstructed signals/images while preserving the low computational complexity of piecewise-linear interpolation. While it clearly outperforms the classical algorithm in terms of quality, it has one negative side effect; namely, the introduction of a Gibbs-like phenomenon (oscillations) when interpolating step-like functions, as mentioned in the literature.⁴ The presence of these oscillations tends to increase the dynamic range of the output image; this effect is especially noticeable in successive interpolation experiments such as multiple image rotations.

Further author information: (Send correspondence to K. Ichige)

K. Ichige: E-mail: koichi@ynu.ac.jp

T. Blu and M. Unser: E-mail: {thierry.blu, michael.unser}@epfl.ch

Both standard and shifted linear interpolation methods employ wavelet-like basis functions that are shifted replicates of a single generator: the “tent” function, which has a central axis of symmetry. In principle, this type of representation can be generalized by introducing multiple generating functions which are not necessarily symmetric anymore. However, to be acceptable from an approximation theoretic point of view, the representation should preserve the “partition of unity” property; more generally, it should allow for the perfect reconstruction of linear polynomials.⁵ The question that we address in this paper is whether or not there are advantages to switching to representations with multiple generators for the task of signal/image interpolation.

We will do so by considering a generalized piecewise-linear model whose knots are not necessarily equally spaced nor symmetrically placed. The underlying model, however, remains regular in the sense that the distribution of the knots follows a periodic pattern. In this context, it is of great interest to determine the optimal placement of the knots so that the interpolation error is minimized. Interestingly, we will see in the case of two generators that the optimal placement of the knots is not at the sampling locations, nor that they should necessarily be equally spaced.

We will first start from a generalized model of multiple piecewise-linear generators, and describe the special case of two generators in detail. Then we evaluate the approach with respect to the specific task of signal/image interpolation. Then we will apply the method to image interpolation and compare its various versions with the traditional approach. This will allow us to determine the optimal parameters values for best performance according to two criteria: (1) maximum PSNR (Peak Signal-to-Noise Ratio), and (2) minimization of the Gibbs-like oscillations. With respect to this last item, we found that the prefiltering (decomposition) scheme could be implemented by FIR filters for a certain range of parameter values, which essentially gets rid of this problem.

2. PROBLEM FORMULATION

Consider a sequence of samples $f[n] = f(nT)$ sampled from a function $f(x)$ with the sampling interval T . In case of one basis function $\varphi(x)$, the interpolation function $f_T(x)$ reconstructed from the samples $f[n]$ is given by a linear combination of shifted basis functions as

$$f_T(x) = \sum_{n \in \mathbf{Z}} c[n] \varphi\left(\frac{x}{T} - n\right), \quad (1)$$

In (1), $c[k]$ denotes the weight parameter that are obtained by enforcing interpolation condition $f_T(nT) = f(nT)$:

$$c[n] = b_\varphi^{-1} * f[n],$$

where

$$\sum b_\varphi^{-1}[n] z^{-n} = \frac{1}{\sum \varphi[n] z^{-n}}.$$

In case of q basis functions $\{\varphi_j(x)\}_{j=0}^{q-1}$, the interpolated function $f_T(x)$ is given by a linear combination of qT -shifted basis functions as

$$f_T(x) = \sum_{k \in \mathbf{Z}} \sum_{j=0}^{q-1} c_j[k] \varphi_j\left(\frac{x}{T} - kq\right) = \sum_{k \in \mathbf{Z}} \mathbf{c}[k]^T \boldsymbol{\phi}\left(\frac{x}{T} - kq\right) \quad (2)$$

where \mathbf{c}_k and $\boldsymbol{\phi}(x)$ respectively denote the weight vector and the basis vector as

$$\begin{aligned} \mathbf{c}[k] &= [c_0[k], c_1[k], \dots, c_{q-1}[k]]^T, \\ \boldsymbol{\phi}(x) &= [\varphi_0(x), \varphi_1(x), \dots, \varphi_{q-1}(x)]^T. \end{aligned}$$

The objective of this paper is first to establish the prefiltering relations in the multiple generator case, and then to investigate whether interpolation quality can be improved by using multiple basis functions instead of one.

3. GENERALIZED PIECEWISE-LINEAR MULTIPLE GENERATORS

This section develops the concept of piecewise-linear interpolation with multiple generators, and studies the case of two generators in detail.

3.1. General Principle

We first start from q different basis functions: $\phi_0(x), \phi_1(x), \dots, \phi_{q-1}(x)$. Hereafter, the sampling interval T is set to be one for the simplicity.

For integer values of x , (2) is reduced to

$$f(n) = \sum_{k \in \mathbf{Z}} \mathbf{c}[k]^T \phi(n - kq). \quad (3)$$

The Discrete-time Fourier transform (DTFT) of (3) can be written as

$$F(e^{-j\omega}) = \mathbf{B}_\varphi(e^{-j\omega})^T \mathbf{C}(e^{-jq\omega}) \quad (4)$$

where

$$\begin{aligned} F(e^{-j\omega}) &= \sum_{n \in \mathbf{Z}} f(n) e^{-jn\omega}, \\ \mathbf{B}_\varphi(e^{-j\omega}) &= \sum_{n \in \mathbf{Z}} \phi(n) e^{-jn\omega}, \\ \mathbf{C}(e^{-jq\omega}) &= \sum_{k \in \mathbf{Z}} \mathbf{c}[k] e^{-jqk\omega}, \end{aligned}$$

In (4), $F(e^{-j\omega})$ and $\mathbf{B}_\varphi(e^{-j\omega})$ are 2π -periodic in ω , and $\mathbf{C}(e^{-jq\omega})$ is $2\pi/q$ -periodic in ω . Thus, if we substitute $\omega = \omega, \omega + 2\pi\frac{1}{q}, \dots, \omega + 2\pi\frac{q-1}{q}$ in (4), $\mathbf{C}(e^{-jq\omega})$ remains unchanged. Then we can rewrite the q -corresponding equations in the following matrix form:

$$\begin{bmatrix} F(e^{-j\omega}) \\ F(e^{-j(\omega+2\pi\frac{1}{q})}) \\ \vdots \\ F(e^{-j(\omega+2\pi\frac{q-1}{q})}) \end{bmatrix} = \left[\mathbf{B}_\varphi(e^{-j\omega}), \mathbf{B}_\varphi(e^{-j(\omega+2\pi\frac{1}{q})}), \dots, \mathbf{B}_\varphi(e^{-j(\omega+2\pi\frac{q-1}{q})}) \right]^T \mathbf{C}(e^{-jq\omega}). \quad (5)$$

Therefore, the DTFT $\mathbf{C}(e^{-jq\omega})$ of the coefficients \mathbf{c}_k can be derived by

$$\mathbf{C}(e^{-jq\omega}) = \left[\mathbf{B}_\varphi(e^{-j\omega}), \mathbf{B}_\varphi(e^{-j(\omega+2\pi\frac{1}{q})}), \dots, \mathbf{B}_\varphi(e^{-j(\omega+2\pi\frac{q-1}{q})}) \right]^{-T} \begin{bmatrix} F(e^{-j\omega}) \\ F(e^{-j(\omega+2\pi\frac{1}{q})}) \\ \vdots \\ F(e^{-j(\omega+2\pi\frac{q-1}{q})}) \end{bmatrix}. \quad (6)$$

A filterbank implementation of this equation is shown in Fig. 1, where the prefilters $\tilde{\Phi}(z) = [\tilde{\Phi}_0(z), \tilde{\Phi}_1(z), \dots, \tilde{\Phi}_{q-1}(z)]^T$ and the reconstruction filters $\Phi(z) = [\Phi_0(z), \Phi_1(z), \dots, \Phi_{q-1}(z)]^T$ are given by

$$\begin{aligned} [\tilde{\Phi}(z), \tilde{\Phi}(e^{-j2\pi\frac{1}{q}}z), \dots, \tilde{\Phi}(e^{-j2\pi\frac{q-1}{q}}z)] &= \frac{1}{q} \left[\mathbf{B}_\varphi(z), \mathbf{B}_\varphi(e^{-j2\pi\frac{1}{q}}z), \dots, \mathbf{B}_\varphi(e^{-j2\pi\frac{q-1}{q}}z) \right]^{-T}, \\ [\Phi(z), \Phi(e^{-j2\pi\frac{1}{q}}z), \dots, \Phi(e^{-j2\pi\frac{q-1}{q}}z)] &= \left[\mathbf{B}_\varphi(z), \mathbf{B}_\varphi(e^{-j2\pi\frac{1}{q}}z), \dots, \mathbf{B}_\varphi(e^{-j2\pi\frac{q-1}{q}}z) \right]. \end{aligned}$$

For a certain class of basis functions, the determinant of the matrix in (5) becomes a delay ($e^{-jq\omega}$) which is the necessary and sufficient condition for the prefilters $\tilde{\Phi}(z)$ to be FIR.

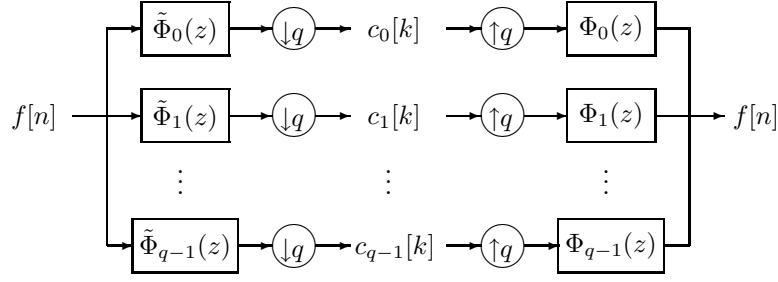


Figure 1. Filterbank construction of the proposed scheme with q generators.

3.2. Case of Two Basis Functions

Here we consider the case of two generating piecewise-linear functions φ_0 and φ_1 . The representation of those functions can be dissymmetric but mirror to each other to satisfy the “partition of unity” as in Fig.2, i.e.

$$\varphi_0(x) = \begin{cases} \frac{x - \tau}{\alpha}, & \tau - 1 \leq x < \tau + \alpha - 1 \\ \frac{2 + \tau - x}{2 - \alpha}, & \tau + \alpha - 1 \leq x < \tau + 1 \\ 0, & \text{otherwise} \end{cases}$$

$$\varphi_1(x) = \begin{cases} \frac{x - \tau - \alpha}{2 - \alpha}, & \tau + \alpha - 1 \leq x < \tau + 1 \\ \frac{\tau + \alpha + 2 - x}{\alpha}, & \tau + 1 \leq x < \tau + \alpha + 1 \\ 0, & \text{otherwise} \end{cases}$$

which reconstructs a signal by

$$f[n] = \sum_{k \in \mathbf{Z}} c_0[k] \varphi_0[n - 2k] + \sum_{k \in \mathbf{Z}} c_1[k] \varphi_1[n - 2k].$$

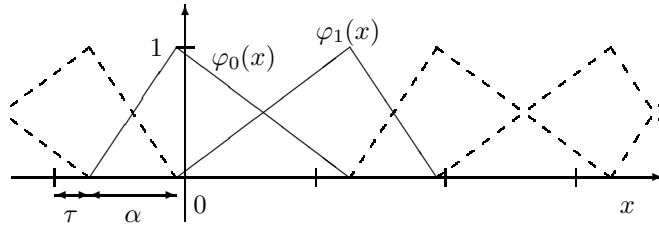


Figure 2. Basis functions

The parameters τ and α correspond to the shift and the dissymmetry, respectively. For any $x \in \mathbf{R}$, the basis functions satisfy the partition of unity:

$$\sum_{n \in \mathbf{Z}} \{\varphi_0(x - 2n) + \varphi_1(x - 2n)\} = 1.$$

If $\tau + \alpha < 1$, the prefilters and the reconstruction filters can be derived using the frequency domain approach developed in the previous subsection. In this case, the matrix in (5) can be written as

$$\begin{aligned} & \left[\mathbf{B}_\varphi(e^{-j\omega}), \mathbf{B}_\varphi(e^{-j(\omega+\pi)}) \right]^T \\ &= \begin{bmatrix} \varphi_0(0) + \varphi_0(1)e^{-j\omega} & \varphi_1(0) + \varphi_1(1)e^{-j\omega} \\ \varphi_0(0) - \varphi_0(1)e^{-j\omega} & \varphi_1(0) - \varphi_1(1)e^{-j\omega} \end{bmatrix} \\ &= \frac{1}{2-\alpha} \begin{bmatrix} (1+\tau) + \tau e^{-j\omega} & (1-\tau-\alpha) + (2-\tau-\alpha)e^{-j\omega} \\ (1+\tau) - \tau e^{-j\omega} & (1-\tau-\alpha) - (2-\tau-\alpha)e^{-j\omega} \end{bmatrix} \end{aligned}$$

which leads the FIR expressions of the reconstruction filters $\Phi_0(z)$ and $\Phi_1(z)$ as

$$\begin{aligned} \Phi_0(z) &= \frac{(1+\tau) + \tau z^{-1}}{2-\alpha}, \\ \Phi_1(z) &= \frac{(1-\tau-\alpha) + (2-\tau-\alpha)z^{-1}}{2-\alpha}, \end{aligned}$$

The inverse of the matrix in (6) can be derived as

$$\begin{aligned} & \left[\mathbf{B}_\varphi(e^{-j\omega}), \mathbf{B}_\varphi(e^{-j(\omega+\pi)}) \right]^{-T} \\ &= \frac{1}{\left[\mathbf{B}_\varphi(e^{-j\omega}), \mathbf{B}_\varphi(e^{-j(\omega+\pi)}) \right]^T} \begin{bmatrix} \varphi_1(0) - \varphi_1(1)e^{-j\omega} & -\varphi_1(0) - \varphi_1(1)e^{-j\omega} \\ -\varphi_0(0) + \varphi_0(1)e^{-j\omega} & \varphi_0(0) + \varphi_0(1)e^{-j\omega} \end{bmatrix} \\ &= \frac{1}{2} \begin{bmatrix} (2-\tau-\alpha) - (1-\tau-\alpha)e^{j\omega} & (2-\tau-\alpha) + (1-\tau-\alpha)e^{j\omega} \\ -\tau + (1+\tau)e^{j\omega} & -\tau - (1+\tau)e^{j\omega} \end{bmatrix} \end{aligned}$$

which also leads the FIR expressions of the prefilters $\tilde{\Phi}_0(z)$ and $\tilde{\Phi}_1(z)$ as

$$\begin{aligned} \tilde{\Phi}_0(z) &= (2-\tau-\alpha) - (1-\tau-\alpha)z, \\ \tilde{\Phi}_1(z) &= -\tau + (1+\tau)z. \end{aligned}$$

The prefilters $\tilde{\Phi}_0(z)$ and $\tilde{\Phi}_1(z)$ can also be derived by time domain calculation based on the recursive equations:

$$\begin{aligned} f[2n] &= \frac{1+\tau}{2-\alpha}c_0[n] + \frac{1-\tau-\alpha}{2-\alpha}c_1[n], \\ f[2n+1] &= \frac{\tau}{2-\alpha}c_0[n] + \frac{2-\tau-\alpha}{2-\alpha}c_1[n]. \end{aligned}$$

Also, the reconstruction filters $\Phi_0(z)$ and $\Phi_1(z)$ can be computed based by

$$\begin{aligned} c_0[n] &= (2-\tau-\alpha)f[2n] - (1-\tau-\alpha)f[2n+1], \\ c_1[n] &= -\tau f[2n] + (1+\tau)f[2n+1]. \end{aligned}$$

The whole process can be drawn in a filterbank form as in Fig.3.

If $\tau + \alpha \geq 1$, the prefilters $\tilde{\Phi}_0$ and $\tilde{\Phi}_1$ become

$$\begin{aligned} \tilde{\Phi}_0(z) &= \frac{(2-\alpha)(1-\tau-\alpha) + \tau(2-\tau-\alpha)z}{(1-\tau)(2-\tau-\alpha) + \tau(1-\tau-\alpha)z^{-2}}, \\ \tilde{\Phi}_1(z) &= \frac{-\tau\alpha z + (2-\alpha)(1-\tau)z^2}{(1-\tau)(2-\tau-\alpha) + \tau(1-\tau-\alpha)z^{-2}}; \end{aligned}$$

they are implemented by Forward/Backward IIR filtering.

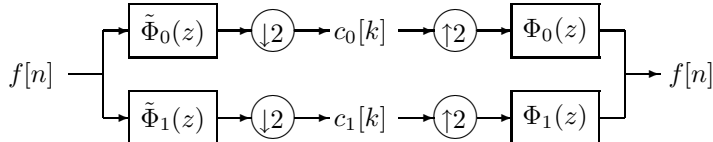


Figure 3. Filterbank construction of the proposed scheme with two generators.

4. SIMULATION

In this section, we evaluate the proposed scheme of two piecewise-linear generators through some simulations.

Similarly to the literature,⁴ we first evaluate the functions through 15 successive image rotations by 24° . The target images are as shown in Figs.5–7(a) which have different characteristics: “Lena” mainly has low frequency components, “Baboon” contains every frequency component and “Particles” is a binary image and regarded as an extreme example.

We tested various combinations of values of the parameters τ and α for those three images to see which combination is the most suitable. Fig.8 depicts the behavior of PSNRs for various values of the parameters τ and α . From Fig.8, we can see that the case of the shifted-linear interpolation ($\tau = 0.21, \alpha = 0$) was the best for all of three images with respect to PSNR. Indeed the reconstructed images are sharp as shown in Figs.5–7(c), much more precise than in the case of standard linear interpolation in Figs.5–7(b).

In Fig.8, we also find that there is another local optimum PSNR around $\tau = 0.21$ and $\alpha = 0.58$. The PSNR here is a little bit lower than that in the shifted-linear case, but the reconstructed images have almost the same quality as shown in Figs.5–7(c),(d). The maximum and minimum values of the reconstructed images are very wide in the shifted-linear case, and are closer to the original in the local optimum case as listed in Table 1. As we see in Fig.6(c), there are some white and black pixels like impulse noise. The values of these pixels are very far from the original range, they are the very reason of data in Table 1.

Table 1. Maximum and minimum values of the original and rotated images

	Lena	Baboon	Particles
	Min/Max	Min/Max	Min/Max
Original	0/255	6/227	0/255
Linear	0/255	6/227	0/255
Shifted-Linear	−105/369	−31/384	−420/1015
Proposed ($\tau = 0.21, \alpha = 0.58$)	−50/343	−5/245	−200/410

The wide range in the shifted-linear interpolation is a consequence of its Gibbs-like oscillations when interpolating step-like functions. Figure 4 shows the result of interpolating a unit step function. Shifted-linear interpolation causes oscillation for several steps. In the local optimum case ($\tau = 0.21$ and $\alpha = 0.58$), there are two possible behaviors (a) and (b) due to two different basis functions. The oscillation in (a) is smaller than that in Shifted-linear, and the case (b) does not make any oscillation. They lead to the smaller range in Table 1.

Computation time for the proposed scheme is almost the same with that for the shifted-linear interpolation, if the processes for c_0 and c_1 in Fig.3 can be executed in parallel.

5. CONCLUDING REMARKS

In this paper, a concept of generalized piecewise-linear multiple generators and its applications have been presented. The present multiple basis functions can be regarded as generalized piecewise linear interpolators. We also developed a scheme of decomposition and reconstruction of signals/images by two dissymmetric piecewise

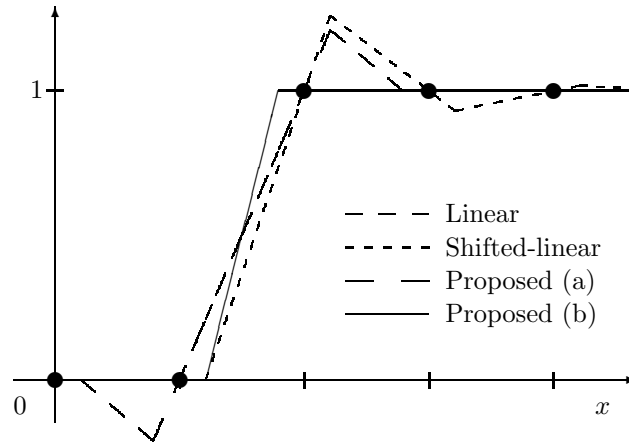


Figure 4. Interpolation of a unit step function.

linear basis functions in a form of a filterbank. Then the scheme was evaluated through computer simulation of digital image rotation.

The error in interpolation and the optimum values of the parameters must be further studied mathematically.

REFERENCES

1. P. Thévenaz, T. Blu and M. Unser, "Image Interpolation and Resampling," in *Handbook of Medical Imaging, Processing and Analysis*, I.N. Bankman Ed., pp. 393-420. Academic Press, San Diego, CA, U.S.A, 2000.
2. P. Thévenaz, T. Blu and M. Unser, "Interpolation Revisited," *IEEE Trans. Med. Imag.*, vol. 19, no. 7, pp. 739-758, July 2000.
3. T. Blu and M. Unser, "Approximation Error for Quasi-Interpolators and (Multi-)Wavelet Expansions," *Appl. Comput. Harmon. Anal.*, vol. 6, no. 2, pp. 219-251, March 1999.
4. T. Blu, P. Thévenaz and M. Unser, "How A Simple Shift Can Significantly Improve The Performance of Linear Interpolation," *Proc. IEEE Int'l Conf. on Image Proc.*, pp. III.377-III.380, Rochester, NY, U.S.A, Sep. 2002.
5. G. Strang, T. Nguyen, *Wavelet and Filter Banks*, Wellesley Cambridge Pr., MA, USA, 1996.

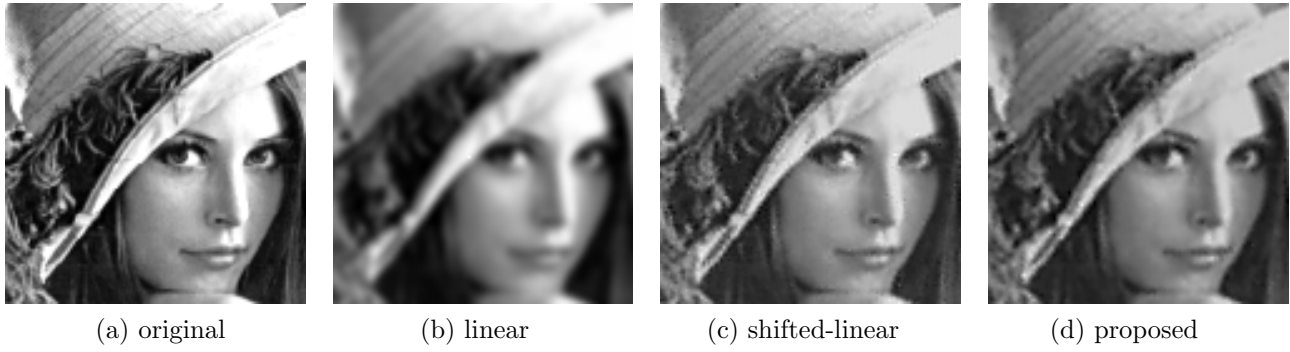


Figure 5. Rotated Images of “Lena”

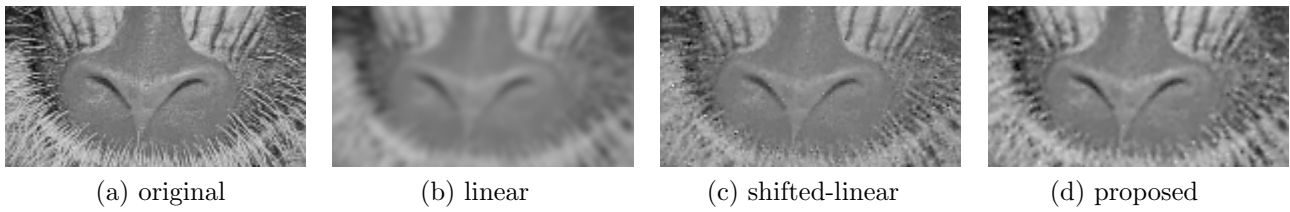


Figure 6. Rotated Images of “Baboon”

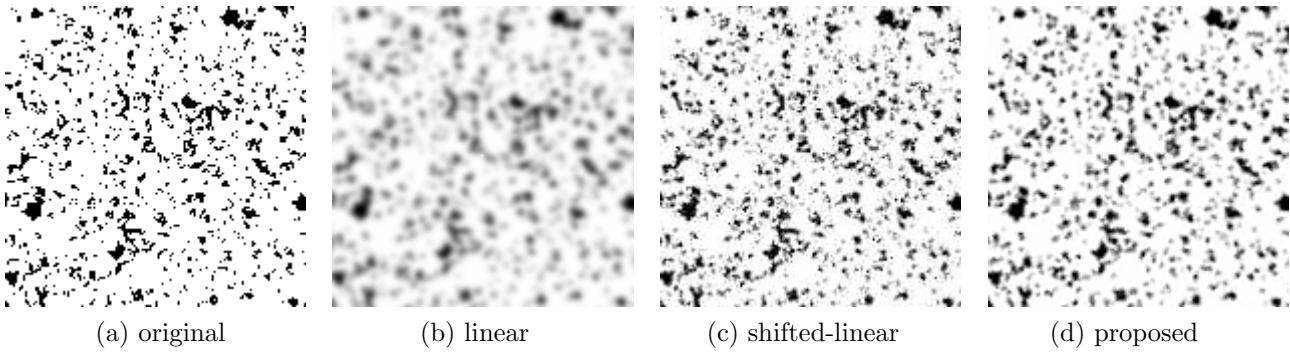
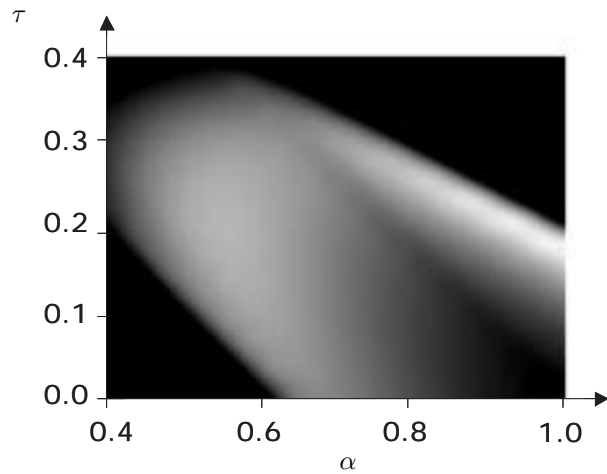
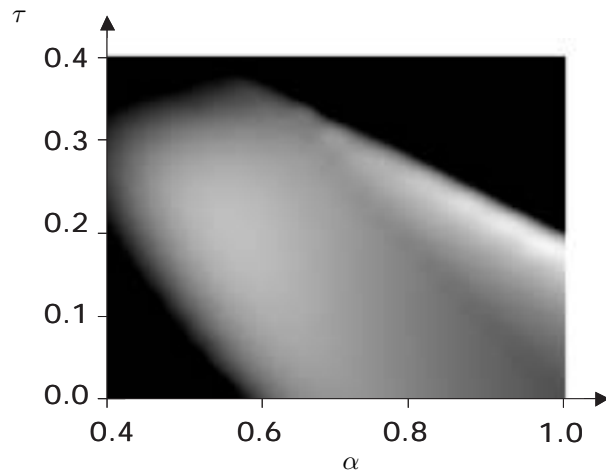


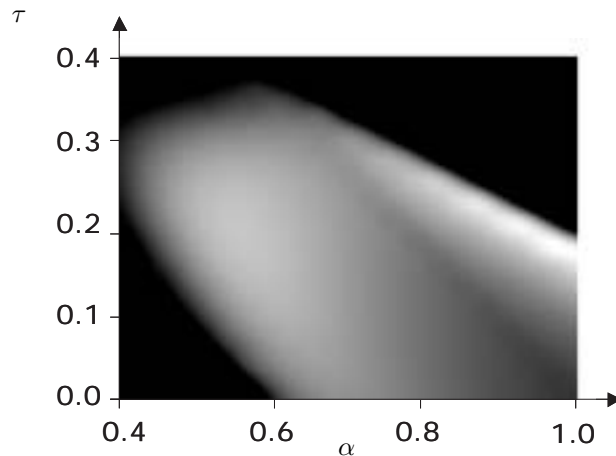
Figure 7. Rotated Images of “Particles”



(a) Lena; white=28dB, black=22dB or less
 Linear: 22.0dB, Shifted-Linear: 28.1dB,
 Proposed: 27.6dB



(b) Baboon; white=18.5dB, black=15dB or less
 Linear: 16.2dB, Shifted-Linear: 18.6dB,
 Proposed: 18.0dB



(c) Particles; white=13.5dB, black=10dB or less
 Linear: 10.6dB, Shifted-Linear: 13.3dB, Proposed: 12.8dB

Figure 8. PSNRs of the rotated images for various combinations of parameters α and τ . Note that the optimum solution is obtained in white regions.